Determining aboveground biomass of the forest successional chronosequence in a test-site of Brazilian Amazon through X- and L- band data analysis

João Roberto Santos*[a], Camila Valéria de Jesus Silva [a], Lênio Soares Galvão [a], Robert Treuhaft [b], José Claudio Mura [a], Soren Madsen [b], Fábio Guimarães Gonçalves [c], Michael Maier Keller [d]

[a] National Institute for Space Research, Av. dos Astronautas, 1758, São José dos Campos, Brazil, [b] Jet Propulsion Laboratory, California Institute of Technology, 4800 Oak Grove Drive, Pasadena, CA, 91109, USA, [c] The Woods Hole Research Center, 149, Woods Hole Road, MA, 02540, USA, [d] USDA Forest Service, Rio Piedras, PR, 100745, USA and University of New Hampshire, Durham, NH 03824, USA.

ABSTRACT

Secondary succession is an important process in the Amazonian region with implications for the global carbon cycle and for the sustainable regional agricultural and pasture activities. In order to better discriminate the secondary succession and to characterize and estimate the aboveground biomass (AGB), backscatter and interferometric SAR data generally have been analyzed through empirical-based statistical modeling. The objective of this study is to verify the capability of the full polarimetric PALSAR/ALOS (L-band) attributes, when combined with the interferometric (InSAR) coherence from the TanDEM-X (X-band), to improve the AGB estimates of the succession chronosequence located in the Brazilian Tapajós region. In order to perform this study, we carried out multivariate regression using radar attributes and biophysical parameters acquired during a field inventory. A previous floristic-structural analysis was performed to establish the chronosequence in three stages: initial vegetation regrowth, intermediate, and advanced regrowth. The relationship between PALSAR data and AGB was significant ($p<0.001$) and results suggested that the "volumetric scattering" (**P**v) and "anisotropy" (**A**) attributes were important to explain the biomass content of the successional chronosequence ($R^2_{adjusted}$ = 0.67; RMSE = 32.29 $Mg.ha^{-1}$). By adding the TanDEM-derived interferometric coherence (γ_i) into the regression modeling, better results were obtained ($R^2_{adjusted}$ = 0.75; RMSE = 28.78$Mg.ha^{-1}$). When we used both the L- and X-band attributes, the stock density prediction improved to 10.8 % for the secondary succession stands.

Keywords: biomass, secondary succession, PALSAR/ALOS, TanDEM/TerraSAR-X, Amazon forest, monitoring.

1. INTRODUCTION

Several natural or human-induced disturbances exert impacts on the world's forests and carbon cycle. Disturbances are the main drivers altering forest structure, creating landscape mosaics, and setting the initial conditions for successional dynamics and structural development [1]. More than 60% of the world's 4 billion ha of forest are recovering from a past disturbance, and 3% of the world's forests are presently disturbed annually by logging, fire, weather, and others factors [2]. .The expansion of agricultural and cattle raising activities has been the most important cause of recent forest loss, accounting for 80% of the worldwide deforestation, primarily through conversion of tropical forests [3]. Thus, the forests could be a net sink or source of carbon depending upon anthropogenic pressure and the management practices.

Forest secondary succession is an important process in the Amazonian region with implications for global carbon cycle and ecosystem changes [4, 5]. It also impacts sustainable regional agriculture because the farmers cut these regrowth areas rather than primary forests, during the shifting cycle of the crop plantations and/or pasture. After land abandonment, the complex landscapes composed of these small farm fields and forest patches under different levels of succession are commonly observed in tropical deforested areas [6]. Based on previous studies about tropical secondary succession [7, 8, 9, 10], the differences in the histories of land use prior to abandonment, the distance to primary forests and the availability of

Second International Conference on Remote Sensing and Geoinformation of the Environment (RSCy2014), edited by Diofantos G. Hadjimitsis, Kyriacos Themistocleous, Silas Michaelides, Giorgos Papadavid, Proc. of SPIE Vol. 9229, 92291E · © 2014 SPIE · CCC code: 0277-786X/14/$18 · doi: 10.1117/12.2066031

seed dispersers, are anticipated to lead to variability in regeneration pathways and the capability of forests to recover tree species diversity and biomass.

Knowledge of the structure, distribution, and biomass of the world's forests is improving rapidly because of the advances in regional and global Earth observation systems and data analysis techniques [11]. Three-dimensional remote sensing allows estimate of the forest canopy height, biomass and carbon stocks [2, 11]. Currently, remote sensing technologies with standardized field information are also addressing ecological issues from forest successional chronosequence and its land-cover changes [12, 13, 14]. However, satellite data and current methods to estimate the extent and age of regenerating tropical forests are still difficult because of the spectral similarities between some successional stages or the smooth transition between them [5, 15, 16].

The Synthetic Aperture Radar (SAR) orbital data, with ability to acquire all-weather images covering large areas with different look angles, resolutions and polarizations, are considered particularly useful for forest monitoring and biomass retrieval. Optical data, although very effective for foliage biomass retrieval, are not suitable for direct retrieval of the woody biomass [17]. Generally, the radar signal at high frequencies (X- and C-bands) is dominated by scattering by the crown layer consisting of foliage and the branches, while the signal response at lower frequencies (L- and P-bands) by the scattering involving major woody biomass components, trunks and branches. Significant correlations between C, L, P-bands radar attributes and the forest structure parameters were found by [18, 19, 20]. The radar backscattering forest models show dependence on the spatial distribution and size of trees [21], biomass content, orientation of trunks, branches and foliage, local topography [22] and also, the baseline of imagery. For forest cover mapping and volume and biomass estimations, three basic approaches based on SAR data [23] are used: backscatter, coherence, and phase-based approaches. One should remember that there are certain effects in the relationship between the radar-signal and structural components of the secondary successional stands (e.g., roughness of targets and humidity content) that should be also considered. The SAR interferometric techniques, such as repeat–pass or single pass interferometry (InSAR) and polarimetric interferometry (PolInSAR), can also provide detailed information about three-dimensional primary and secondary forest structure of the scattering targets under study [24, 25].

In 2012, the tropical America presented 380,000 Km^2 of secondary forests [26]. A recent study in the Brazilian Amazon [27] indicated that the secondary forest had an area of 129,000 Km^2. This information has stimulated the scientific community to develop new remote sensing tools to support monitoring policies of forest succession chronosequence. Due to the importance of the natural vegetation regrowth types in restoration of degraded tropical environments through the accumulation of biomass, the build up of organic matter, the maintenance of biodiversity and of hydrological regime, and also the atmospheric carbon fixation, the use of radar remote sensing to accurately differentiating them into different stages is valuable for better understanding their role and their relationships with the Amazon forest landscape change. Thus, the objective of this study is to verify the capability of the full polarimetric PALSAR/ALOS (L-band) attributes, when combined with the interferometric coherence (γ_i) from the TanDEM/TerraSAR (X-band), to characterize the different stages of secondary succession and to improve the AGB estimates of the successional chronosequence located in the Brazilian Tapajós region.

2. MATERIAL AND METHODS

Area under study

The study area is located in the Tapajós region (NW Pará State, Brazil), delimited by the geographical coordinates S $2^0$53'11.63" - $3^0$13'20.22" and W $54^0$53'20.69" - $55^0$04'53.31". It has been extensively studied by several researchers [19, 28, 29]. The regional climate is AmW (Köeppen classification) with average values of annual precipitation and temperature of 2,300 mm and 26°C, respectively. This region is characterized by a low rolling relief, constituting the lower Amazon plateau and the upper Xingu-Tapajós Plateau. The predominant soil type is Xanthic Acrustox (USA Soil Taxonomy). This study area is dominated by a continuous cover of primary tropical rainforest characterized by the presence of emergent trees (Dense Ombrophilous Forest), as well as sections of low to dissected plateaus with few emerging individuals and a high density of palm trees (Open Ombrophilous Forest). The land use is related to subsistence agriculture, a few cash crops, raising cattle and selective logging activities. Some areas after agricultural and pasture practices are abandoned and left to regenerate.

Acquisition of SAR and forest inventory data

The images from PALSAR (Phased-Array L-band Synthetic Aperture Radar), onboard the Advanced Land Observing Satellite (ALOS), were acquired on 13 March 2009 in the PLR 1.1 multipolarimetric mode (single look complex image) and utilized for the extraction of polarimetric attributes. They were obtained from an ascending orbit with an incidence angle of 24° and a slant and azimuth resolution of 9.36 m and 3.58 m, respectively. By using the TanDEM-X (TerraSAR-X add-on for Digital Elevation Measurement) satellite with the almost identical twin-satellite TerraSAR-X, the first satellite-based single-pass SAR interferometer was formed. Because of the simultaneous operation mode of both satellites, the disturbing effect of temporal decorrelation is limited to a minimum level because of the small along-track baseline between the SAR sensors [30, 31]. In the present study, we used the interferometric data of 22 September 2011 with the following characteristics: stripmap mode, dual polarization (HH/HH), single look slant range complex, pixel resolution of 1.42 m (range) and 2.54 m (azimuth). To obtain the interferometric coherence (γ_i), considering those variations in resolution in the range (horizontal) and along-track (vertical) directions, the average of the set of pixels representative of each typology was calculated (35 pixels in range and 20 in azimuth). This comprised areas of 50 x 50 m each. This value was approximately equivalent, on the TanDEM image, to the maximum size adopted to perform inventory in the field plots (0.25 ha).

Polarimetric and radiometric calibrations [32] and a resampling procedure (*multi-look*) in the PALSAR/ALOS images were initially performed on these images, followed by the application of the modified Lee filter [33] with a window size of 5 x 5 pixels. After that, the extraction of backscatter values (σ°) in the HH, HV, VV polarizations was obtained. Then, the conversion procedure of complex scattering matrix [S] into covariance [C] and coherence [T] matrices was performed, from which attributes comprising different radar polarimetric characteristics that express the specific behavior to each forest target were calculated. The following incoherent SAR attributes, which are based on information from the real part of each pixel, were considered in data analysis: backscatter coefficient (σ°) [34]; the ratio of parallel polarization (Rp) and cross polarization (Rc) [35]; the indices, formulated by [36], referred to biomass index (BMI), canopy structure index (CSI) and volume scattering index (VSI); and also the radar forest degradation index (RDFI) proposed by [37]. On other hand, several coherent attributes that take advantage of SAR phase information, were evaluated: the polarimetric coherence of HH-VV (γ) and phase difference of HH-VV ($\Delta\varphi$), described by [35]; parameters resulting from the target decomposition [38] by the coherence matrix [T], named entropy (H), anisotropy (A) and the mean alpha angle ($\bar{\alpha}$); the volume scattering components (*Pv*), double bounce (Pd) and surface (Ps), resulting from the decomposition matrix [C] [39]; the magnitude (αs) and Touzi phase (Φαs) as well as the orientation angle (ψ) and helicity (τ_m), also derived from the same former decomposition [40].

On its turn, from the TanDEM and TerraSAR-X data, the InSAR-derived interferometric coherence (γ_i,), was obtained. This attribute represents the modulus of the correlation coefficient between them [41] and is calculated through the equation:

$$\left| \rho_{\gamma i} \right| = \frac{\left| \langle S_1 \, S_2^* \rangle \right|}{\sqrt{\langle |S_1|^2 \rangle \, \langle |S_2|^2 \rangle}} \tag{1}$$

where $\rho_{\gamma i}$ = complex correlation coefficient; S_1 = signal received by the antenna at one end of the baseline; S_2 = signal received by the antenna at the other end.

Due to the volume decorrelation caused by vegetation, which is a result from multiple scattering occurring in the radar signal interaction with the forest target, the interferometric coherence can be used to obtain more information on forest structure. Therefore, this attribute has the potential to improve the estimation of biomass. The coherence ranges from 0 to 1, representing the structural complexity of the vegetation. The maximum value is assigned to the vegetation which produces a signal that vertically compact. Smaller coherence values indicate more vertically distributed powers, possibly due to vertically more distributed vegetation, with more widely spaced elements and greater average height. Some studies have assessed the potential of interferometric coherence in the analysis of forest biophysical parameters [30, 42].

All these SAR attributes were extracted in ROIs representing each thematic class, properly georeferenced and inventoried in the field survey to measure the biophysical parameters that served to model the biomass through generic [43] and specific [44] allometric equations. Each field plot ranged from 0.10 to 0.25 ha in area, where all trees with diameter at breast height (DBH) above 10 cm for advanced secondary succession and DBH > 5 cm for intermediate and initial secondary succession were measured. Besides the DBH, the total height of trees was measured in each sample. Furthermore, the species were identified and the scientific and family names were confirmed using the "Brazilian Species Name Index 2013" (http://floradobrasil.jbrj.gov.br/) together with the database from the Missouri Botanical Garden 2013 (http://www.tropicos.org). In order to represent the floristic and structural variability of the successional chronosequence in the Tapajós study area, face to their radar signal response, 25 plots totaling a sample area of 5.5 ha were inventoried.

Multiple regression analysis was employed to assess the sensitivity of the PALSAR polarimetric attributes and the interferometric coherence of TanDEM-X to variations in forest biomass. This regression model was adjusted using Ordinary Least Squares (OLS). The previous selection of explanatory variables, based on the inspection of the correlation matrix, was carried out using also the "best subset" procedure. The performance of the model was verified from the analysis of R^2, $R^2_{adjusted}$, RMSE and Cp Mallow criteria, as well as from some other statistical procedures such as the diagnosis of multi-colinearity (by calculation of Variance Inflation Factor – VIF), analysis of outliers (Cook´s distance) and residuals [45]. The last phase of the methodological procedure was the validation of the generated model using a hold-out set of samples [45].

3. RESULTS AND DISCUSSIONS

Characterization of secondary succession types

Knowledge of the regeneration process of secondary forests in the tropical region must be based on chronosequence studies, whose definition involves several distinct sites, referring to the time elapsed since the abandonment or the disturbance. It must present: a similarity of soil types and environmental conditions within the same climate zone and submitted in the past to the same land use [26]. At the studied Tapajós test-site, most areas under a succession process are small fragments, within primary forests (with or without timber exploitation) or agricultural areas and pasture.

Considering a floristic-structural analysis of this chronological sequence, the following succession phases were discriminated: Initial – SSI (<6 years of vegetation regeneration), Intermediate – SSInt (6-15 years) and Advanced – SSA (>15 years). During the inventory of 5.5 ha, 943 trees were identified, totaling 221 species distributed among 48 families. The species richness (S) presented values of 84, 145 and 158 at the succession trajectory, while the Shannon-Weaver (H') index presented values of 2.95, 3.8 and 4.34 for the above mentioned phases, respectively. The Shanon (H') index delivers more information about the composition of the community that only the measure of richness (S), because it represents both the abundance and the homogeneity of species. A higher H' value represents a diverse and equally distributed community. Species *Cecropia palmata* Willd., *Banara guianensis* Aubl., and *Vismia guianensis* (Aubl.) Pers. dominate the younger successional stage, presenting IVI values of 16.44, 13.84 and 10.32 respectively. At the intermediate stage the following species occur: *Annona exsucca* DC., *Casearia grandiflora* Cambess., *Cecropia palmata* Willd, and *Aparisthmium cordatum* (A. Juss.) Baill, with IVI values of 5.65, 4.96, 4.42 and 4.43, respectively. At the advanced succession, there is a dominance the species *Inga alba* (Sw.) Willd., *Cordia scabrifolia* A. DC., *Jacaranda copaia* (Aubl.). D. Don., and *Cecropia sciadophylla* Mart., with IVI values of 5.58, 4.64, 4.42 and 3.66, respectively. The *Fabaceae* family presented most abundance and richness at all chronological sequence stages, as expected in the Amazon region [46], except for the initial succession, only with richness, but with abundance only of families *Salicaceae* and *Urticaceae*. During the advanced stage, the richest one in species, almost 50% of the trees belong to families *Fabaceae, Urticaceae, Boraginaceae, Lecythidaceae* and *Annonaceae.*

For the structural analysis of the successional chronosequence, at the initial natural regrowth, those trees with DBH >5 cm have average diameter and height values of 8.28 cm and 8.15 m respectively, presenting an average biomass of 14.59 ± 4.37 (ton.ha^{-1}). At the intermediate secondary succession the trees have an average DBH of 12.69 cm and a height of 11.64 m, with a biomass of 56.34 ± 3.77 ton.ha^{-1}. At the advanced regrowth (DBH >10 cm) these values reached an

average 21.02 cm of DBH and 16.27m height, and a biomass of 107.50 ± 5.82 ton.ha^{-1}, respectively. The regrowth rates vary differentially with the spatial and time scales, with multiple succession trajectories, reflecting the fragmentation level of the landscape, the edaphic conditions, in addition to the differences in earlier land use. It is important to mention that primary forests also inventoried in this study have an average biomass of 340.56 ± 10.22 ton.ha^{-1}, demonstrating that there is still a long time for resetting the chronological sequence of carbon content in the area under study

Multi radar-remote sensing data for modeling the aboveground biomass of regrowth areas

Initially an evaluation was made on the potential of coherent and incoherent attributes derived from L-band PALSAR at the biomass estimation, using the statistical regression analysis method. The first order model fitting to predict *Y* (Biomass) from secondary succession was made based on the following equation:

$$Yi = \beta_0 + \beta_1 Xi_1 + \beta_2 Xi_2 + ... + \beta p_{-1} Xi,p_{-1} + \varepsilon_i \quad (2)$$

where Y_i is the value of the dependent variable, the log of aboveground biomass, for the i_{th} observation; $\beta_o, \beta_1, \beta_2,..., \beta_{p-1}$ are the parameters of the model; $X_{i1}, X_{i2}, ..., X_{i,p-1}$ are the values of the p-1 explanatory radar-variables for the i_{th} observation; and ε_i is a random error term with mean $E\{\varepsilon_i\} = 0$ and variance $\sigma^2\{\varepsilon_i\} = \sigma^2$.

This model fitting was initially tested with a total of 23 coherent and incoherent attributes, obtained from PALSAR full-polarimetric data, mentioned at item 2 from this work, whose values were extracted from 25 ROIs, representative of several stages of secondary succession. Afterwards, in this biomass modeling the variable interferometric coherence (γ_i), derived from TanDEM/TerraSAR-X data, was included in the biomass modeling.

Based on the series of statistical parameters which included R^2, $R^2_{adjusted}$, RMSE, Cp Mallow and Variance Inflation Factor, the best model for biomass estimation was obtained with PALSAR/ALOS data (Figure 1a) in areas of successional chronosequence ($R^2 = 0.70$; $R^2adj = 0.67$), as follows:

$$log\ AGB = 0.701 + 5.153 * Pv - 1.454 * A \quad (3)$$

where log AGB is the logarithmic mode of aboveground biomass; *Pv,* is the volumetric scattering derived from the Freeman-Durden target decomposition model; and variable A is the Anisotropy.

On the other hand, with the joint participation of the HH-pol of interferometric coherence attribute(γ_i) from TanDEM/TerraSAR-X and PALSAR (L-band) attributes, the best regression model (Figure 1b) to estimate the biomass (with values of 0.78 and R^2adj of 0.75) is expressed by:

$$log\ AGB = 2.963 - 2.5359 * \gamma_i + 5.26954 * Pv \quad (4)$$

where: log AGB is the logarithmic mode of aboveground biomass; γ_i is the interferometric coherence*;* and *Pv,* is the volumetric scattering derived from Freeman-Durden target decomposition model.

At the statistical parameters (Table 1) generated at these regressions, one verifies that the values of Variance Inflation Factor (VIF) for the independent variables, of both models selected, were low. This confirms that there is no multi-colinearity among the independent variables.

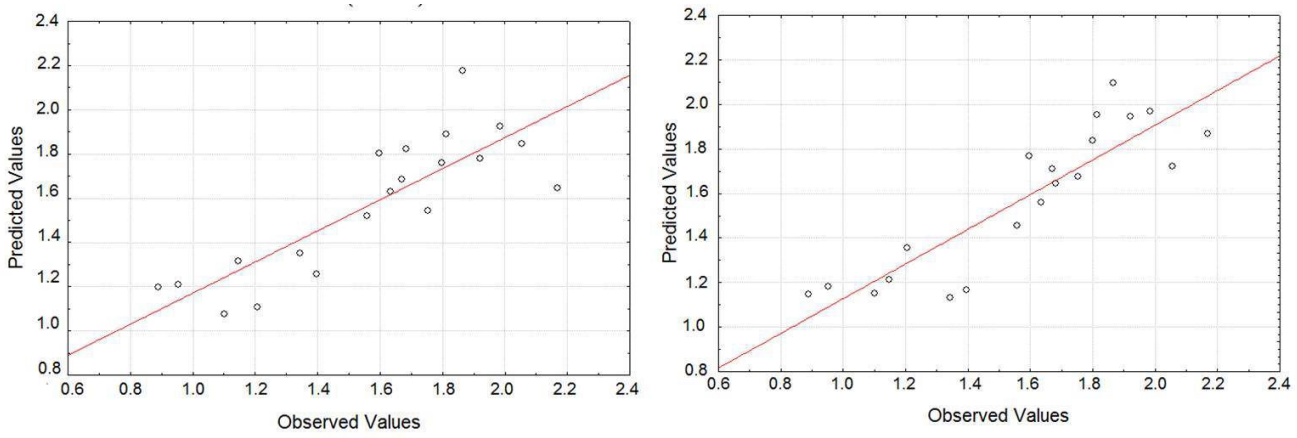

Figure 1. Estimated vs. ground-observed biomass (in log) of secondary succession for PALSAR L-band model (left); and PALSAR combined with TanDEM X- band dataset (right).

Table 1. Independent variables for each model selected and its respective partial R^2 regression coefficients (with standard deviations and *p-value*) and also, the Variance Inflation Factor (VIF) values.

Treatment	Model					
	Independent variable	Parcial R^2	Coefficient	SE	p- values	VIF
PALSAR	Intercept	-	0.701	0.339	0.054291	-
	Pv	0.73	5.153	1.164	0.000369	1.439123
	A	-0.31	-1.454	1.076	0.194562	1.439123
PALSAR + TanDEM	Intercept	-	2.963	0.931	-	-
	γ_i	-0.57	-2.5359	0.882	0.010547	1.097827
	Pv	0.82	5.2695	0.877	0.000014	1.097827

The inclusion of variable (γ_i) in the regression model contributed to the estimation of AGB without generating a redundancy of information. The residuals of both models, plotted on a diagram in relation to the forecasted AGB values, showed homogeneity in its distribution, including also at the Shapiro-Wilk test, at 0.05 the significance level.

From the correlation analysis among all 23 previous radar attributes, it was found out that the interferometric coherence (TanDEM-X/TerraSAR) obtained an *r* value, almost twice as high as that one of polarimetric coherence - γ_p- of PALSAR. This is due to the higher sensitivity of γ_i referring to the arboreal components in each succession stage, while γ_p is more sensitive to the orientation and form of these components [42]. The density of arboreal individuals in the secondary succession, its arrangement in the strata of each succession stage (one stratum in the youth phase; two or three strata, according to the regeneration period advances) is perceived differently by the radar with different frequencies and imaging modes, even if this measure is expressed in AGB. As an example of the correlation level among the variables considered in both models, one verifies that the spatial arrangement of the response occupied by *Pv* and γ_i against the *log* of biomass, corresponds to each one of the 25 plots of secondary succession (Figure 2).

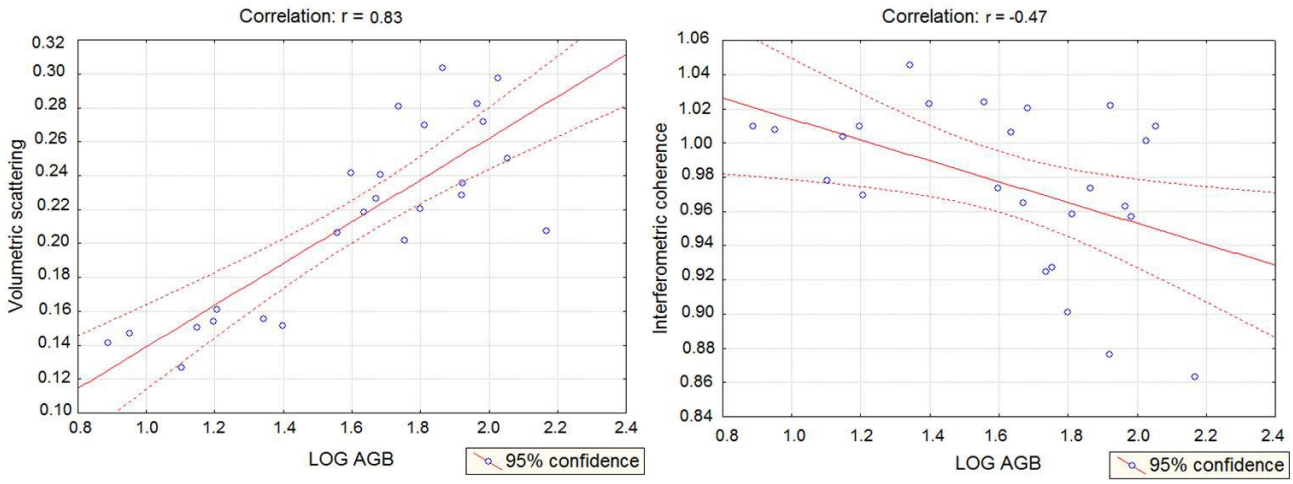

Figure 2. Correlation diagram between biomass (in log) and the variables of volumetric scattering (PALSAR), and of HH- pol interferometric coherence (TanDEM) from tropical secondary succession.

From a detailed analysis of both attributes (*Pv* and γ_i) for the successional chronosequence, we verified that: (a) the volume scattering components values, obtained from the Freeman and Durden target decomposition model, increased with the advancement of the vegetation regrowth from 0.1995 ± 0.0504 (initial succession) to 0.2294 ± 0.0528 (the advanced one); (b) there was an inverse tendency referring to the interferometric coherence, as expected, whereby the initial regrowth presented values of 0.9909 ± 0.0503 that decreased to 0.9708 ± 0.0424 at the advanced regeneration. It is important to mention that the primary tropical forest in the Tapajós region presented interferometric coherence values of 0.8147 ± 0.1376. Deciduous, coniferous and mixed forests present values of 0.851± 0.044, 0.823 ± 0.066 and 0.842 ± 0.052 of the HH-pol mean of interferometric coherence magnitude (TanDEM-X) [47]respectively.

4. CONCLUSIONS

At more refined analysis, derived from the generation of these two regression models, one concludes that the volumetric scattering, among all PALSAR (L-band) attributes, had the highest incremental predictive power at the statistics of the regressions found. However, adding the interferometric coherence at band X, the stock density prediction of the model improved by 10.8 % for the secondary succession stands. The polarimetric and interferometric attributes (in L- and X-bands) can be together a significant option for the improvement of AGB estimates, especially because they are sensitive to the variations of the vertical structure of forest typology. This occurs mainly in succession stages, which present lower biomass values than in tropical forests, as shown in this study. The differences among coherence statistics were related to the intensity of volume scattering, which was more significant at coniferous forests with less homogeneous structure.

5. AKNOWLEDGMENTS

The authors are grateful to the Coordenação de Aperfeiçoamento de Pessoal de Nível Superior (CAPES), the Conselho Nacional de Desenvolvimento Científico e Tecnológico (CNPq), the Jet Propulsion Laboratory and California Institute of Technology (under a contract with National Aeronautics and Space Administration – task number 281945.02.61.02.82) and the Instituto Chico Mendes de Conservação da Biodiversidade (ICMBio/MMA - Sisbio Process 35010-1 and 38157-2). Thanks are also due to Museu Paraense Emílio Goeldi – MPEG for the botanical assistance and Large Scale Biosphere-Atmosphere Experiment in Amazonia (LBA-Santarém Office) for the logistic support during the field surveys. We thank the German Aerospace Center (DLR) for processing and delivery of the TanDEM-X data.

REFERENCES

[1] Swanson, M.E., Franklin, J.F., Beschta, R.L., Crisafulli, C.M., DellaSala, D.A., Hutto, R.L., Lindenmayer, D.B. and Swanson, F.J., " The forgotten stage of forest succession: early-successional ecosystems on forest sites," Front. Ecol. Environ. 9 (2), 117-125 (2011).

[2] Pan, Y., Birdsey, R. A., Phillips, O.L. and Jackson, R.B., "The structure, distribution, and biomass of the World's Forests," Annu. Rev. Ecol. Evol. Syst. 44, 593-622 (2013).

[3] Gibbs, H.K., Brown, S., Niles, J.O. and Foley, J.A., "Monitoring and estimating tropical forest carbon stocks: making REDD a reality," Environ. Res. Lett. 213, 054023 (2007).

[4] Foody, G.M., Palunbiskas, G., Lucas, R.M., Curran, P.J. and Honzak, M., "Identifying terrestrial carbon sinks: classification of successional stages in regenerating tropical forest from Landsat TM data," Rem. Sens. Environ. 55, 205-216 (1996).

[5] Neeff, T., Graça, P. M. D., Dutra, L. V. and Freitas, C.D., "Carbon budget estimation in Central Amazonia: successional forest modeling from remote sensing data," Rem. Sens. Environ. 94 (4), 508-522 (2005).

[6] Quesada, M., Sanchez-Azofeifa, G.A., Alvarez-Anorve, M., Stoner, K.E., Avila-Cabadilla, L., Calvo-Alvarado, J., et al., "Succession and management of tropical dry forests in the Americas: review and new perspectives," For. Ecol. Managem. 258(6), 1014-1024 (2009).

[7] Lucas, R.M., Honzák, M., Amaral, I. D., Curran, P. J. and Foody, G. M., "Forest regeneration on abandoned clearances in central Amazonia," Int. J. Rem. Sens. 23(5), 965–988 (2002).

[8] Fearnside, P.M., "Deforestation in Brazilian Amazonia: History, rates, and consequences," Cons. Biol. 19(3), 680-688 (2005).

[9] Davidson, E.A., de Carvalho, C.J.R., Figueira, A.M., Ishida, F.Y., Ometto, J.P.H.B., Nardoto, G.B., Saba, R.T., Hayashi, S.N., Leal, E.C., Vieira, I.C.G. and Martinelli, L.A., "Recuperation of nitrogen cycling in Amazonian forests following agricultural abandonment," Nature 447(7147), 995-998 (2007).

[10] Prates-Clark, C. C., Lucas, R. M. and Santos, J. R., "Implications of land-use history for forest regeneration in the Brazilian Amazon," Can. J. Rem. Sens. 35(6), 534-553 (2009).

[11] Treuhaft, R.N., Law, B.E. and Asner, G.P., "Forest attributes from radar interferometric structure and its fusion with optical remote sensing," BioSc. 54 (6), 561-571 (2004).

[12] Castro, K. L., Sanchez-Azofeifa, G.A. and Rivard,B., "Monitoring secondary tropical forests using space-borne data: implications for Central America," Int J. Rem. Sens. 24(9), 1853-1894 (2003).

[13] Lu, D., Mausel, P., Brondízio, E. and Moran, E. "Classification of successional forest stages in the Brazilian Amazon basin," For. Ecol. Manag. 181(3), 301-312. (2003).

[14] Galvão, L.S., Breunig, F.M., Santos, J. R. and Moura, Y. M., "View-illumination effects on hyperspectral vegetation indices in the Amazonian tropical forest," Int. J. Appl. Earth Observ. and Geoinf. 21, 291-300 (2013).

[15] Neeff, T., Lucas, R.M., Santos, J.R., Brondizio, E.S. and Freitas, C.C., "Area and age of secondary forests in Brazilian Amazonia 1978-2002: An empirical estimate," Ecosystems 9(4), 609-623 (2006).

[16] Sánchez-Azofeifa, G. A., Castro-Esau, K. L., Kurz, W. A. and Joyce, A., "Monitoring carbon stocks in the tropics and the remote sensing operational limitations: from local to regional projects," Ecol. Appl. 19(2), 480-494 (2009).

[17] Sader, S. A., Wide, R. B., Lawrence, W. T. and Joyce, A. T., "Tropical forest biomass and successional age class relationships to a vegetation index derived from landsat TM data," Rem. Sens. Environ. 28, 143-198 (1989).

[18] Le Toan,T., Beaudoin, A., Riom, J. and Guyon, D., "Relating forest biomass to SAR data,".IEEE Trans. Geosc. Rem. Sens., 30(2), 403-411 (1992).

[19] Santos, J. R., Araujo, L. S., Freitas, C. C., Soler, L. S., Gama, F. F. and Dutra, L.V., "Analysis of forest biomass variation in the Amazon and its' influence on the response of P-band SAR polarimetric data,". Proc. of SPIE 4879, 252-259 (2003).

[20] Kumar, S., Pandey, U., Kushwaha, S. P., Chatterjee, R. S. and Bijker, W., "Aboveground biomass estimation of tropical forest from Envisat advanced synthetic aperture radar data using modeling approach," J. Appl Rem. Sens., 6, 1-18 (2012).

[21] Neeff, T.; Biging, G. S.; Dutra, L. V.; Freitas, C. C. and Santos, J. R., "Modeling spatial tree pattern in the Tapajós forest using interferometric height," Rev. Brasil. Cartog., 57(1), 1-6 (2005).

[22] Bispo, P. C., "Efeitos da geomorfometria na caracterização florístico-estrutural da Floresta Tropical na região de Tapajós com dados SRTM e PALSAR, " Tese de Doutorado - INPE, 147 (2012).

[23] Koch, B. "Status and future of laser scanning, synthetic aperture radar and hyperspectral remote sensing data for forest biomass assessment," ISPRS Journ. Photog. Rem. Sens., 65, 581-590 (2010).

[24] Treuhaft, R. N., Chapman, B. D., Santos, J. R., Gonçalves, F. G., Dutra, L. V., Graça, P. M. L. A. and Drake, J. B., "Vegetation profiles in tropical forests from multibaseline interferometric synthetic aperture radar, field, and lidar measurements," J. Geophys. Res. 114, D23110 (2009).

[25] Treuhaft, R. N., Gonçalves, F. G., Drake, J. B., Chapman, B. D.; Santos, J.R., Dutra, L. V., Graça, P. M. L. A. and Purcell, G. H., "Biomass estimation in a tropical wet forest using Fourier transforms of profiles from lidar or interferometric SAR," Geophys. Res. Let., 37(23) L23403 (2010).

[26] OIMT - Organización Internacional de las Maderas Tropicales., "Directrices de la OIMT para la restauración, ordenación y rehabilitación de bosques tropicales secundarios y degradados," OIMT - Serie de Politicas Forestales, 13, 97. (2002).

[27] Almeida, C.A., Pinheiro, T.F., Barbosa, A.M., Abreu, M.R.B.S., Lobo, F.L., Silva, M., Gomes, A.R., Sadeck, L.W.R., Medeiros, L.T.B., Neves, M.F., Silva, L.C.T. and Tamasauskas, P.F.L.F., "Metodologia para mapeamento de vegetação secundária na Amazônia Legal,".Instituto Nacional de Pesquisas Espaciais, 32 (2009).

[28] Aragão, L.E.O.C., Shimabukuro, Y.E., Espírito Santo, F.D.B. and Williams, M., "Landscape pattern and spatial variability of leaf area index in Eastern Amazonia," For. Ecol. Manag. 211(3), 240-256 (2005).

[29] Galvão, L. S., Ponzoni, F. J.; Liesenberg, V. and Santos, J. R., "Possibilities of discriminating tropical secondary succession in Amazônia using hyperspectral and multiangular CHRIS/PROBA data," Int J. Appl. Earth Observ. and Geoinf., 11(1), 8-14 (2009).

[30] Krieger, G., Moreira, A., Fiedler, H., Hajnsek, I., Werner, M., Younis, M. and Zink, M., "TanDEM-X: A satellite formation for high resolution SAR interferometry," IEEE Trans. Geosc. Rem. Sens., 45(11), 3317-3341 (2007).

[31] Askne, J.I.H., Fransson, E.S., Santoro, M., Soja, M.J. and Ulander, L.M.H., "Model-based biomass estimation of a Hemi-Boreal Forest from multitemporal TanDEM-X acquisitions," Remote Sens*., 5*, 5574-5597 (2013).

[32] Shimada, M., Member, S., Isoguchi, O., Tadono, T. and Isono, K., "PALSAR radiometric and geometric calibration,". IEEE Trans. Geosc. Rem. Sens**.**, 47(12), 3915–3932 (2009).

[33] Lee, J.; Grunes, M. R.; Grandi, G., Member, S., "Polarimetric SAR speckle filtering and its implication for classification," IEEE Trans. Geosc. Rem. Sens., 37(5), 2363-2373 (1999).

[34] Woodhouse, I. H., "Introduction to microwave remote sensing," Boca Raton: Taylor & Francis Group CRC Press,. 370 (2006).

[35] Henderson, F.M. and Lewis, A.J., "Manual of remote sensing**:** principles and applications of imaging radar," John Wiley Sons, New York, USA, 896p. (1998).

[36] Pope, K.O., Benayas-Rey, J.M. and Paris, J.F., "Radar remote sensing of forest and wetland ecosystems in the Central American tropics," Rem. Sens. Environ., 48(2), 205-219 (1994).

[37] Saatchi, S. S.; Marlier, M.; Chazdon, R. L.; Clark, D. B.and Russel, A. E.,"Impact of spatial variability of tropical forest structure on radar estimation of aboveground biomass, "Rem. Sens. Environ., 115(11), 2836-2849 (2011).

[38] Cloude, S.R. and Pottier, E., "A review of target decomposition theorems in radar polarimetry," IEEE Trans. Geosc. Rem. Sens., 34(2), 498-518 (1996).

[39] Freeman, A. and Durden, S.L., "A three-component scattering model for polarimetric SAR data," IEEE Trans. Geosc. Rem. Sens., 36(3), 963-973 (1998).

[40] Touzi, R., "Target scattering decomposition in terms of roll-invariant target parameters," IEEE Trans. Geosc. Rem. Sens., 45(1), 73-84 (2007).

[41] Martone, M., Brautigam, B., Rizzoli, P., Gonzalez, C.; Bachmann, M. and Krieger, G., "Coherence evaluation of TanDEM-X interferometric data," ISPRS Journ. Photogr. Rem. Sens., 73, 21-29 (2012).

[42] Treuhaft, R. N. and Siqueira, P. R., "Vertical structure of vegetated land surfaces from interferometric and polarimetric radar,". Radio Science, 35(1), 141-177 (2000).

[43] Uhl, C.; Buschbacher, R. and Serrão, E. A. S., "Abandoned pastures in Eastern Amazonia. I . Patterns of plant succession," Journ. Ecology, 76(3), 63-681 (1988).

[44] Nelson, B. W., Mesquita, R., Pereira, J. L. G., De Souza, S. G. A., Batista, G. T. and Couto, L.B., "Allometric regressions for improved estimate of secondary forest biomass in the central Amazon," For. Ecol. Manag**.**, 117 (1), 149-167 (1999).

[45] Kutner, M. H., Nachtsheim, C. J.; Neter, J. and Li, W., "Applied Linear Statistical Models," Boston McGraw- Hill/Irwin, 1396. (2005).

[46] Ter Seege, H., Pitman, N. C. A, Sabatier, D., Baraloto, C.; Salomão, R. P.; Guevara, J.E.,Phillips, O. L., Castilho, C. V, Magnusson, W. E.; Molino, J. F., Monteagudo, A., Núñez Vargas, P., Montero, J. C., Feldpausch, T. R., Coronado, E. N. H., Killeen, T. J., Mostacedo, B., Vasquez, R., Assis, R. L. *et al.*, *"*Hyperdominance in the Amazonian tree flora,". Science, 342(6156), 325-334 (2013).

[47] Demirpolat, C. X-band interferometric radar for mapping temporal variability in forest. Thesis of MSc. degree. Aalto University- Finland. 86. (2012).